Theory of Interactions of Non-Relativistic Flavor-Mixed Particles and its possible Implications to the Physics of Dark Matter and the Cosmic Neutrino Background

By

Alexander L. Ford

Submitted to the Department of Physics and Astronomy and the
Faculty of the Graduate School of the University of Kansas
in partial fulfillment of the requirements for the degree of
Master of Science

Mikhail V. Medvedev, Chairperson

Committee members

Thomas E. Cravens

Hume A. Feldman

Date defended: 12/3/2012

The Thesis Committee for Alexander L. Ford certifies
that this is the approved version of the following thesis :

Theory of Interactions of Non-Relativistic Flavor-Mixed Particles and its possible Implications to the Physics of Dark Matter and the Cosmic Neutrino Background

Mikhail V. Medvedev, Chairperson

Date approved: 12/3/2012

Abstract

The existence of flavor-mixed particles is well established. We discuss the dynamics of a stable particle with flavor mixing scattering off of a weak potential. We demonstrate that conversion from one mass state to another is possible through scattering and calculate the associated differential cross sections. The mass conversion is not analogous to flavor oscillations or particle decay. The implications of mass conversion, in general, and with respect to flavor-mixed dark matter and the cosmic neutrino background (CνB) is discussed.

Contents

List of Figures

List of Tables

Chapter 1

Flavor-Mixed Particles

1.1 Introduction

The universe is full of many different particles, some of which have an interaction (flavor) basis that is non-diagonal in the propagation (mass) basis. A classical particle has a well defined mass and well defined interaction properties. In contrast, a quantum particle with a certain flavor may not have a defined mass. A flavor-mixed particle is a linear combination of mass eigenstates. Stated another way, $|f_\alpha\rangle = C_1|m_a\rangle + C_2|m_b\rangle + ...$, where $|f\rangle$ and $|m\rangle$ denote flavor and mass eigenstates and C_1, C_2 are complex constants. Likewise, a mass eigenstate is a superposition of flavor eigenstates. The list of massive flavor-mixed particles includes particles such as: quarks, kaons, b-mesons, and neutrinos. Lets look at the neutrino as an example of a stable flavor-mixed particle. Neutrinos come in 3 flavors: electron, muon, and tau; and each flavor is a linear combination of three mass eigenstates: m_1, m_2, m_3. As a neutrino propagates, the mass eigenstates move with different velocities, which cause time-dependent interference in the flavor basis (flavor oscillations). Flavor oscillations is a property of all massive flavor-mixed particles. Most of the research on the dynamics of flavor-mixed particles has looked at stable relativistic particles. These mixed particles remain coherent in the flavor basis. This is because the coherence length is a

function of velocity: $L_{\text{coh}} = \sigma|\mathbf{v}_1 + \mathbf{v}_2|/|\mathbf{v}_1 - \mathbf{v}_2|$. For atmospheric neutrinos created by the interaction of cosmic rays with the Earth atmosphere, $L_{coh} \simeq 6 \times 10^{22}$ km $\simeq 2$ Gpc [1]. However, if a mixed particle is non-relativistic, then it will become incoherent and split into its mass basis. In general, mass states – represented by wave packets, hence having a finite spatial extent – traveling with different velocities separate spatially over time and cause flavor oscillation to cease once the mass states no longer overlap, see figure (1.1). Even if the wave packets had identical velocities, flavor coherence is lost over time due to the wave packet spreading and it's dependence on momentum. The mass and flavor eigenstates of flavor-mixed particles are related by the unitary transformation,

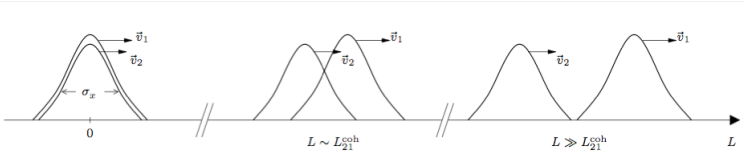

Figure 1.1: Illustration of wave packet separation, taken from [1].

$$|f_i\rangle = \sum_j U_{ij}|m_j\rangle, \tag{1.1}$$

where U is a unitary matrix, and $|m_i\rangle$ and $|f_i\rangle$ are the mass and flavor states respectively. In the simplest case of a two-flavor system, the unitary transformation is the familiar rotation matrix. One transforms the interaction potential from the flavor basis to the mass basis by, $U^\dagger V_f U = V_m$, where $V_f = \text{diag}(V_\alpha, V_\beta)$. The diagonal terms of V_m are $V_{aa} = V_\alpha \cos^2\theta_{12} + V_\beta \sin^2\theta_{12} = 1 - V_{bb}$ and the off-diagonal terms are $V_{ab} = V_{ba} = (V_\alpha - V_\beta)\cos\theta_{12}\sin\theta_{12}$, where θ_{12} is the mixing angle. The potential is non-diagonal in the mass basis; therefore, when a mass state scatters off of the potential, there is a nonzero probability that it scatter into the other mass state. This process has many implications, including scenarios of cold dark matter (CDM) evaporation from halos [2] and dynamics of the cosmic neutrino background(CνB).

1.2 Calculating Scattering Amplitudes

We start with the Schrödinger equation, $i\hbar\frac{\partial}{\partial t}\psi(\mathbf{r},t) = \left(-\frac{\hbar^2}{2m}\bigtriangledown^2 + V(\mathbf{r})\right)\psi(\mathbf{r},t)$, and use separation of variables to split $\psi(\mathbf{r},t)$ into $\psi(\mathbf{r})e^{-iEt/\hbar}$. At $t=-\infty$, a particle with energy E_i travels toward the potential $V(\mathbf{r})$ and at $t=\infty$ the scattered particle has an energy E_f. Assuming the potential is time-independent, integration over all-time yields a δ-function,

$$\int e^{i(E_f-E_i)/\hbar}dt \sim \delta(E_f - E_i), \tag{1.2}$$

which enforces energy conservation. Now using the time-independent Schrödinger equation, $-\frac{\hbar^2}{2m}\bigtriangledown^2\psi + V\psi = E\psi$, one approach to calculate the cross section of a particle scattering off of a spherically symmetric potential is to approximate it as a plane wave and use the Born approximation [3]. For this approximation, one seeks solutions of the form $\psi \approx \exp(ikz) + f(\vartheta)\frac{\exp(ikr)}{r}$. The scattering amplitude, $f(\vartheta)$, tells one the probability of scattering into a direction ϑ and is related to the cross section by $\sigma = \int |f(\vartheta)|^2 d\Omega$, where Ω is the solid angle. Now, defining $k \equiv \sqrt{2mE}/\hbar$ and rewriting the time-independent Schrödinger equation in a more succinct form,

$$(\bigtriangledown^2 + k^2)\psi = \frac{2m}{\hbar^2}V\psi, \tag{1.3}$$

gives the form of the Helmholtz equation. One way to solve it is to use the Green's function approach [4]. The goal is to find a function $G(\mathbf{r})$ with a delta function source,

$$\left(\bigtriangledown^2 + k^2\right)G(\mathbf{r}) = \delta^3(\mathbf{r}). \tag{1.4}$$

Then $\psi(\mathbf{r}) = \int G(\mathbf{r}-\mathbf{r}_0)H(\mathbf{r}_0)d^3\mathbf{r}_0$ with $H(\mathbf{r}) \equiv 2m/\hbar^2 V(\mathbf{r})\psi(\mathbf{r})$. It can be shown that indeed this equation satisfies the Schrödinger equation,

$$\left(\bigtriangledown^2 + k^2\right)\psi(\mathbf{r}) = \int \left(\left(\bigtriangledown^2 + k^2\right)G(\mathbf{r}-\mathbf{r}_0)\right)H(\mathbf{r}_0)d^3\mathbf{r}_0$$
$$= \int \delta^3(\mathbf{r}-\mathbf{r}_0)H(\mathbf{r}_0)d^3\mathbf{r}_0 = \frac{2m}{\hbar^2}V(\mathbf{r})\psi(\mathbf{r}). \quad (1.5)$$

One solves for $G(\mathbf{r})$ using a Fourier transformation to turn the differential equation into an algebraic equation.

$$G(\mathbf{r}) = \frac{1}{(2\pi)^{3/2}}\int e^{i\kappa\cdot\mathbf{r}}g(\kappa)d^3\kappa \quad (1.6)$$

Using $\delta^3(\mathbf{r}) = (2\pi)^{-3}\int e^{i\kappa\cdot\mathbf{r}}d^3\kappa$ and plugging Equation (1.6) into Equation (1.4) yields,

$$\int \left[\left(\bigtriangledown^2 + k^2\right)e^{i\kappa\cdot\mathbf{r}}\right]g(\kappa)d^3\kappa = \frac{1}{(2\pi)^{3/2}}\int e^{i\kappa\cdot\mathbf{r}}d^3\kappa \quad (1.7)$$

After evaluating the Laplacian, one sets the integrands equal to each other,

$$[(-\kappa^2 + k^2)e^{i\kappa\cdot\mathbf{r}}]g(\kappa) = \frac{1}{(2\pi)^{3/2}}e^{i\kappa\cdot\mathbf{r}}, \quad (1.8)$$

and solves for

$$g(\kappa) = \frac{1}{(2\pi)^{3/2}(-\kappa^2 + k^2)}\ . \quad (1.9)$$

Combining Equation (1.9) with Equation (1.6) and evaluating the integral in spherical coordinates with $\mathbf{r}$ along the polar axis yields,

$$G(\mathbf{r}) = \frac{1}{(2\pi)^3}\int e^{i\kappa\cdot\mathbf{r}}\frac{1}{(k^2-\kappa^2)}d^3\kappa = -\frac{e^{ikr}}{4\pi r}\ . \quad (1.10)$$

Using ψ_0 as a free particle, $(\bigtriangledown^2 + k^2)\psi_0 = 0$, the equation for $\psi(\mathbf{r})$ becomes:

$$\psi(\mathbf{r}) = \psi_0 + \int G(\mathbf{r}-\mathbf{r}_0)\frac{2m}{\hbar^2}V(\mathbf{r}_0)\psi(\mathbf{r}_0)d^3\mathbf{r}_0 \quad (1.11)$$

Replacing $G(\mathbf{r}-\mathbf{r}_0)$ with the solution in Equation (1.10),

$$\psi(\mathbf{r}) = \psi_0 - \frac{m}{2\pi\hbar^2}\int \frac{\exp\left(ik|\mathbf{r}-\mathbf{r}_0|\right)}{|\mathbf{r}-\mathbf{r}_0|}V(\mathbf{r}_0)\psi(\mathbf{r}_0)d^3\mathbf{r}_0 \tag{1.12}$$

If one is looking for $\psi(\mathbf{r})$ far away from the scattering center, then an appropriate approximation is $|\mathbf{r}| \gg |\mathbf{r}_0|$. Using this approximation and defining $\mathbf{k} \equiv k\hat{r}$ one can simplify $G(\mathbf{r}-\mathbf{r}_0)$.

$$\frac{e^{ik|\mathbf{r}-\mathbf{r}_0|}}{|\mathbf{r}-\mathbf{r}_0|} \approx \frac{e^{ikr}}{r}e^{-i\mathbf{k}\cdot\mathbf{r}_0} \tag{1.13}$$

Substituting Equation (1.13) into Equation (1.12) yields,

$$\psi(\mathbf{r}) \approx \psi_0 - \frac{e^{ikr}}{r}\frac{m}{2\pi\hbar^2}\int e^{-i\mathbf{k}\cdot\mathbf{r}_0}V(\mathbf{r}_0)\psi(\mathbf{r}_0)d^3\mathbf{r}_0 \tag{1.14}$$

Equation (1.14) is of the form where one can read off the scattering amplitude,

$$f(\vartheta,\phi) = -\frac{m}{2\pi\hbar^2}\int e^{-i\mathbf{k}\cdot\mathbf{r}_0}V(\mathbf{r}_0)\psi(\mathbf{r}_0)d^3\mathbf{r}_0. \tag{1.15}$$

1.3 Scattering off a Flavor Potential

We consider a mass state $|m_i\rangle$ where $i = a, b$ scattering off of an interaction potential and calculate the scattering amplitudes of the interaction. For concreteness, we choose the Yukawa type interaction potential $V_\alpha = \alpha\exp(-\mu_\alpha r)/r$ and $V_\beta = \beta\exp(-\mu_\beta r)/r$, where α and β are the strengths and μ_α^{-1} and μ_β^{-1} are the characteristic spatial extent of the potential. For generality, we assume that $\mu_\alpha \neq \mu_\beta$. However, if the interaction with the potential with both flavors is transmitted by the same boson, then $\mu_\alpha = \mu_\beta$. The wavefunction of the incoming (unscattered) particle can be approximated by a plane wave, which is the exact solution of the Schrödinger equation at infinity, where the interaction potential vanishes, $\mathbf{\Psi}_0(\mathbf{r}) = \psi_0|m_i\rangle$ with $\psi_0(\mathbf{r}) = e^{ik_i\hat{z}}$ and $k_i \equiv \sqrt{2m_iE}/\hbar$, where $|m_a\rangle$ and $|m_b\rangle$ are orthogonal.

One can calculate the scattering amplitudes using Equation (1.15)

$$f(\vartheta,\phi) = -\frac{m_i}{2\pi\hbar^2}\int e^{-i\mathbf{k}_i\cdot\mathbf{r}}V_m(\mathbf{r})\psi_0(\mathbf{r})d^3\mathbf{r}. \tag{1.16}$$

Since $V_m(\mathbf{r})$ is a 2x2 matrix, integration of the matrix elements yields the scattering matrix, S, and $\langle m'|S|m\rangle = f(\vartheta)$ where the primed state signifies after scattering and the unprimed state signifies before scattering. The scattering matrix elements give the probability for an initial mass state to scatter into another mass state.

$$S = \begin{pmatrix} S_{11} & S_{12} \\ S_{21} & S_{22} \end{pmatrix} \Rightarrow \begin{pmatrix} S_{a\to a} & S_{b\to a} \\ S_{a\to b} & S_{b\to b} \end{pmatrix}. \tag{1.17}$$

First, solving for

$$\begin{aligned} S_{11} &= -\frac{m_a}{2\pi\hbar^2}\int e^{-i\mathbf{k}_a\cdot\mathbf{r}}V_{aa}(\mathbf{r})\psi_0(\mathbf{r})d^3\mathbf{r} \\ &= -\frac{m_a}{2\pi\hbar^2}\int e^{ik_a\hat{z}-i\mathbf{k}_a\cdot\mathbf{r}}\left(\frac{\alpha e^{-\mu_\alpha r}}{r}\cos^2\theta_{12}+\frac{\beta e^{-\mu_\beta r}}{r}\sin^2\theta_{12}\right)d^3\mathbf{r} \end{aligned} \tag{1.18}$$

Defining $\mathbf{\Delta k}_i \equiv k_a\hat{z} - \mathbf{k}'_i$ and using spherical coordinates lets one simplify $\exp(i(k_a\hat{z} - \mathbf{k}_a)\cdot\mathbf{r})$ to $\exp(i\Delta k_a r\cos\vartheta)$. The ϕ integral gives a factor of 2π, and the ϑ integral yields $2\sin(\Delta k_a r)/\Delta k_a r$, which only leaves r to integrate over.

$$\int_0^\infty \frac{2\sin(\Delta k_a r)}{\Delta k_a}\left(\alpha e^{-\mu_\alpha r}\cos^2\theta_{12}+\beta e^{-\mu_\beta r}\sin^2\theta_{12}\right)dr \tag{1.19}$$

This procedure is then repeated to solve for the other matrix elements:

$$S_{11} = \frac{-2m_a}{\hbar^2}\left(\frac{\alpha\cos^2\theta_{12}}{\mu_\alpha^2+\Delta k_a^2}+\frac{\beta\sin^2\theta_{12}}{\mu_\beta^2+\Delta k_a^2}\right), \tag{1.20}$$

$$S_{12} = \frac{-m_a}{\hbar^2}\sin(2\theta_{12})\left(\frac{\alpha}{\mu_\alpha^2+\Delta k^2}-\frac{\beta}{\mu_\beta^2+\Delta k^2}\right), \tag{1.21}$$

$$S_{21} = \frac{-m_b}{\hbar^2} \sin(2\theta_{12}) \left(\frac{\alpha}{\mu_\alpha^2 + \Delta k^2} - \frac{\beta}{\mu_\beta^2 + \Delta k^2} \right), \tag{1.22}$$

and

$$S_{22} = \frac{-2m_b}{\hbar^2} \left(\frac{\alpha \sin^2 \theta_{12}}{\mu_\alpha^2 + \Delta k_b^2} + \frac{\beta \cos^2 \theta_{12}}{\mu_\beta^2 + \Delta k_b^2} \right). \tag{1.23}$$

The interaction potential is time independent (energy is conserved) and is stationary (momentum is conserved); therefore, for S_{11} and S_{22} the k of the incoming particle is unchanged in the scattered particle. This lets one simplify $\Delta k_i^2 = 4k_i^2 \sin^2(\vartheta/2)$. S_{11} and S_{22} are the well known elastic scattering amplitude of a particle off a weak interaction potential. However, for S_{12} and S_{21} momentum and energy cannot both be conserved, due to the change in mass and therefore, $\Delta k^2 = k_a^2 + k_b^2 - 2k_a k_b \cos(\vartheta)$ for the off diagonal matrix elements. The interesting matrix elements are the off-diagonals because they lead to mass-eigenstate conversions. Recalling Equation (1.2), there is an energy constraint on mass conversion; namely, $m'^2c^4 \leq m^2c^4 + p^2c^2$. So the complete matrix element is:

$$S = \Theta\left(\Delta(m^2)c^2 + p^2\right) \left(\frac{m' \sin(2\theta_{12})\beta}{\hbar^2\mu_\beta^2 + \hbar^2\Delta k^2} - \frac{m' \sin(2\theta_{12})\alpha}{\hbar^2\mu_\alpha^2 + \hbar^2\Delta k^2} \right) \tag{1.24}$$

where Θ is the heaviside function and $\Delta(m^2) = m^2 - m'^2$. Imagine an initial mass state that has a non-relativistic velocity and is gravitationally bound. This initial state then interacts with an interaction potential and undergoes mass conversion to a lighter state. By conservation of energy, the final state's velocity is larger than the initial bound state. Depending on the mass difference, the final state could have a large enough velocity to escape the potential well [2]. Let the initial state have a mass, m_h, and the final state have a mass, m_l'. The scattering amplitude for this case is

$$S_{h\to l} = m_l \sin(2\theta_{12}) \left(\frac{\beta}{\hbar^2\mu_\beta^2 + \hbar^2\Delta k^2} - \frac{\alpha}{\hbar^2\mu_\alpha^2 + \hbar^2\Delta k^2} \right), \tag{1.25}$$

where $\hbar^2\Delta k^2 = \Delta p^2 = p_h^2 + p_l'^2 - 2p_h p_l' \cos(\vartheta)$. Using conservation of energy,

$$E^2 = m_h^2 c^4 + p_h^2 c^2 = m_l'^2 c^4 + p_l'^2 c^2 \tag{1.26}$$

and solving for $p_l'^2$, one gets the expression

$$p_l'^2 = \Delta m(m_h + m_l')c^2 + p_h^2. \tag{1.27}$$

In general, equation (1.25) is the scattering amplitude for mass conversion, and the differential cross section is $|S_{h\to l}|^2$. It can be illustrative to make assumptions and look at specific scenarios. Since the initial velocity is non-relativistic p_h can be neglected. If one assumes $m_h \approx m'_l \approx m$ and that the final velocity is non-relativistic, then the expression for $p_l'^2$ and v'_l simplify to $2m\Delta mc^2$ and $c\,(2\Delta m/m)^{1/2}$ respectively. Substituting the new expression for p'_l, $\Delta p^2 \approx 2m\Delta m - p_h\sqrt{8m\Delta m}\cos(\vartheta)$, setting $\hbar = 1 = c$:

$$S_{h\to l} = \frac{m'\beta\sin(2\theta_{12})}{\mu_\beta^2 + 2m\Delta m - p_h\sqrt{8m\Delta m}\cos(\vartheta)} - \frac{m'\alpha\sin(2\theta_{12})}{\mu_\alpha^2 + 2m\Delta m - p_h\sqrt{8m\Delta m}\cos(\vartheta)} \tag{1.28}$$

Since $m_h \approx m'_l$, Δm must be small, and therefore one can Taylor expand around a small $\Delta m/m$. Keeping terms linear in $\Delta m/m$ and p_h,

$$\begin{aligned} S_{h\to l} = -m'\sin(2\theta_{12})\left(\frac{\alpha}{\mu_\alpha^2} - \frac{\beta}{\mu_\beta^2}\right) \\ + m'\sin(2\theta_{12})\left(2m\Delta m - p_h\sqrt{8m\Delta m}\cos(\vartheta)\right)\left(\frac{\alpha}{\mu_\alpha^4} - \frac{\beta}{\mu_\beta^4}\right) + O(2) \end{aligned} \tag{1.29}$$

The zeroith order term has no ϑ dependence, which is to be expected for a weak interaction scattering. Assuming that the same gauge boson mediates the interaction, lets one set

$\mu_\alpha = \mu_\beta = \mu$:

$$S_{h\to l} = m' \sin(2\theta_{12}) \frac{\left(2m\Delta m - p_h\sqrt{8m\Delta m}\cos(\vartheta)\right) - \mu^2}{\mu^4} (\alpha - \beta) \,. \tag{1.30}$$

In this form, it is easy to see that if the strengths of each flavor are the same then there will not be mass conversion. Now, if one assumes that v_l is relativistic, then one can still neglect a non-relativistic p_h, but the expression for p'_l changes.

$$m'^2_l c^2 + p'^2_l = m_h^2 c^2 \tag{1.31}$$

$$m'^2_l c^2 + (\gamma m'_l v'_l)^2 = m_h^2 c^2 \tag{1.32}$$

$$\gamma^2 m'^2_l c^2 = m_h^2 c^2 \ . \tag{1.33}$$

Assuming in the relativistic case that $v'_l \approx c$, then $\gamma^2 m'^2_l c^2 \to (\gamma m'_l v'_l)^2$ and $p'_l = m_h c$. Again, substituting the new expression for p'_l into equation (1.25) and setting $\hbar = 1 = c$

$$S_{h\to l} = \frac{m'_l \beta \sin(2\theta_{12})}{\mu_\beta^2 + m_h^2 \left(1 - 2\cos(\vartheta) p_h/m_h\right)} - \frac{m'_l \alpha \sin(2\theta_{12})}{\mu_\alpha^2 + m_h^2 \left(1 - 2\cos(\vartheta) p_h/m_h\right)} \ . \tag{1.34}$$

Since, $p_h \ll m_h$, one can Taylor expand around small p_h/m_h.

$$\begin{aligned} S_{h\to l} = -m' \sin(2\theta_{12}) &\left(\frac{\alpha}{\mu_\alpha^2 + m_h^2} - \frac{\beta}{\mu_\beta^2 + m_h^2}\right) \\ &- 2 p_h m_h m'_l \cos(\vartheta) \sin(2\theta_{12}) \left(\frac{\alpha}{(\mu_\alpha^2 + m_h^2)^2} - \frac{\beta}{(\mu_\beta^2 + m_h^2)^2}\right) \end{aligned} \tag{1.35}$$

Again the zeroith order term does not have a ϑ dependence and the first order term does have a $\cos(\vartheta)$ dependence similar to the non-relativistic case. Further, this result has the same functional form as the non-relativistic case with a renormalized mass of the gauge boson.

Chapter 2

Implications

2.1 Dark Matter

With these scattering amplitudes, one can look at the dynamics of a mixed particle in its mass basis. It has been previously shown [2] that repetitive mass conversions of a system where m_h is gravitationally bound and m_l isn't, can 'evaporate' the gravitational potential, figure (2.1). This 'evaporation' can provide an explanation for the "missing satellite problem" and soften the central cusps in dark matter halos. Currently, an attractive candidate for CDM is the lightest supersymmetric particle, which is required to be stable and is flavor-mixed. Furthermore, if there is high mass degeneracy, then additional particles could become stable due to kinematically forbidden decay channels.

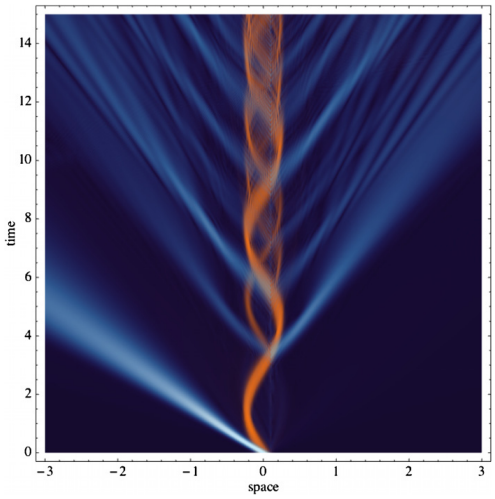

Figure 2.1: The light blue represents a light mass-state and the orange represents a heavy mass-state. There is a scatterer at 0.1, allowing for mass conversion, taken from [2].

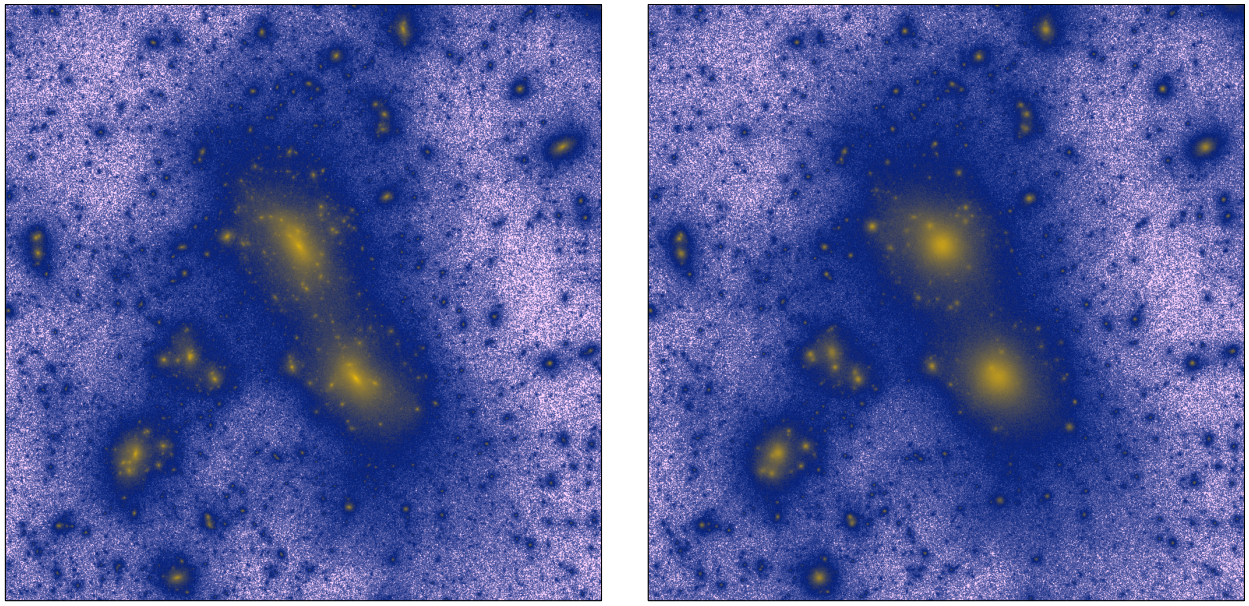

Figure 2.2: The distribution of dark matter in a region of size $5h^{-1}$ Mpc. The classical ΛCDM model is on the left and the two-component flavor-mixed ΛCDM model is on the right. One can see that the amount of small scale structure is much larger on the right. Both simulations involve 1.28×10^8 particles, taken from [5].

2.1.1 Substructure Problem

ΛCDM simulations predict overabundance of small mass halos compared to the number of observed satellite galaxies in the Local Group. Observations show that the number of satellite halos around galaxies of varying luminosity are different. In contrast, simulations show an approximate self-similarity of CDM halos of different masses [6]. To resolve the discrepancy between observation and simulations, an examination of the properties of dark matter is needed. The leading candidate for CDM is the lightest supersymmetric particle (neutralino) which is flavor-mixed; however, other candidates (axions,

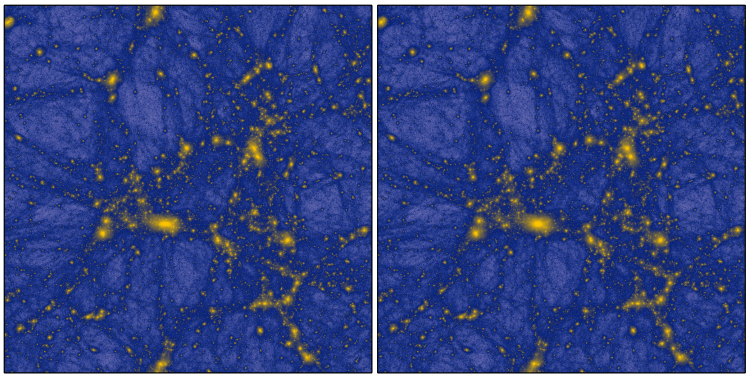

Figure 2.3: The distribution of dark matter in a region of size $50h^{-1}$ Mpc. The classical ΛCDM model is on the left and the two-component flavor-mixed ΛCDM model is on the right. One can see that the large structure match quite well. Figure (2.2) is a zoomed in region located right of center, taken from [5].

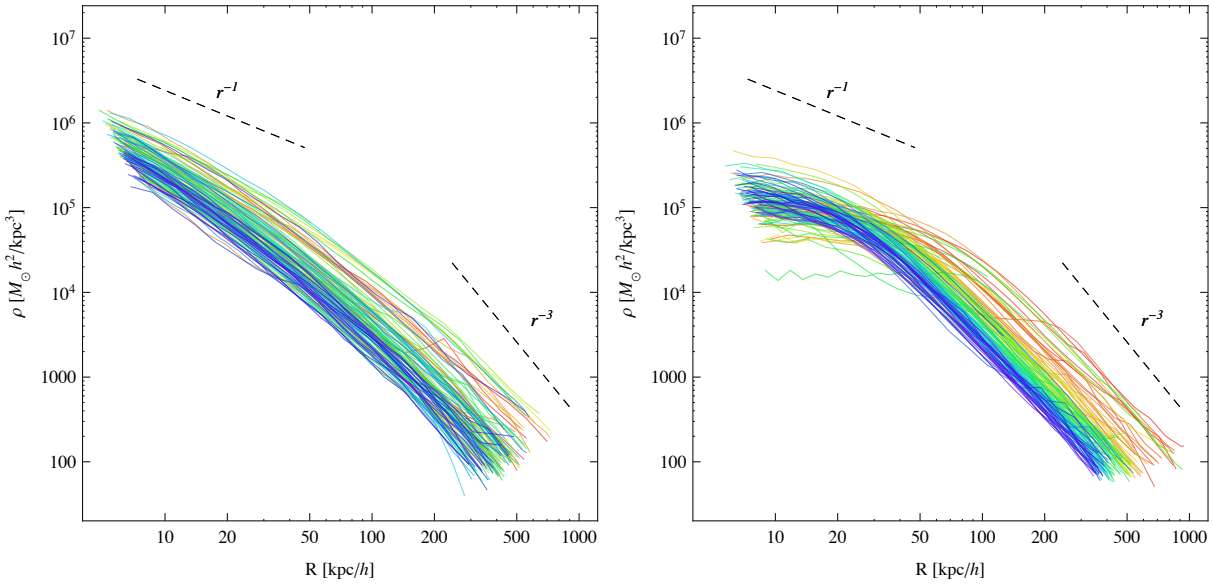

Figure 2.4: Mass density profiles of 12o well-resolved dark matter halos. The classical ΛCDM model is on the left and the two-component flavor-mixed ΛCDM model is on the right. The profiles are color-coded by halo mass, red is the most massive and blue is the least massive. The left plot clearly shows the formation of a soft profile at small radii, taken from [5].

sterile neutrinos, *etc.*) that are flavor-mixed are not excluded. A self-interacting flavor-mixed dark matter particle can scatter and undergo mass conversion, as previously discussed. The velocity required to escape the satellite halos $\ll$ the velocity required to escape the large-mass halos. Therefore, the kinetic energy gained from conversion of a heavy dark matter particle into a lighter one can give the lighter particle enough energy to escape the satellite halos (figure (2.2)), but not enough to escape the large-mass halos (figure (2.3)).

2.1.2 Core-Cusp Problem

The observed rotation velocity associated with dark matter in the inner parts of disk galaxies rises approximately linearly with radius. This gives a constant mass density profile and thus indicates the presence of a central core. ΛCDM simulations give an inner mass density profile that is described by a power law:

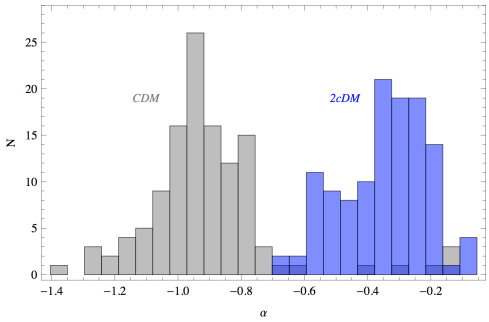

Figure 2.5: A histogram of the slopes of the inner mass density profiles shown in figure (2.4), taken from [5].

$\rho \sim r^{-1}$. This cusp model is in direct conflict with the observations of a core. Very recent galaxy simulations preformed by Medvedev [5] incorporating cold two-component dark matter with flavor-mixing and self-interactions show a mass density profile, $\rho \sim r^{\alpha}$, with α ranging from -0.2 to 0.6 (figure (2.5)), which matches well with current observations, see figure (2.4).

2.2 Cosmic Neutrino Background

Another exciting area where flavor-mixed particles are non-relativistic is the cosmic neutrino background. The CνB is composed of relic neutrinos that underwent freeze out ~ 100 seconds after the big band. Freeze out occurs when the interaction rate of a species is less than the expansion rate.

2.2.1 Energy Difference between Neutrinos and Photons after Electron Positron Annihilation

Photons and neutrinos were in thermal equilibrium after there freeze out and before electron positron annihilation. After e^+e^- annihilation, the photon energy increased and the neutrino energy remained the same. While the neutrinos remain relativistic this will remain the energy difference. The standard derivation of the energy difference is as follows:

$$S \propto g_*(aT)^3 \tag{2.1}$$

where, S is entropy, g_* is the effective degrees of freedom, a is the scale factor, and T is temperature. For the particles in thermal equilibrium with the photons $g_*(aT)^3$ remains constant; therefore the value of aT after $e^{\pm}$ annihilation must be larger than that before $e^{\pm}$ annihilation because the effective degrees of freedom are decreasing. The cubed root of the ratio of g_* before $e^{\pm}$ annihilation ($= 11/2$) to g_* after $e^{\pm}$ annihilation ($= 2$) is equal to the

temperature change [7].

$$\left(\frac{11}{4}\right)^{1/3} = \frac{T_\gamma}{T_\nu} \approx 1.4 \tag{2.2}$$

This temperature split is only valid while the neutrinos remain ultra-relativistic, meaning they can be accurately approximated as massless. As the neutrinos' energy falls, the temperature difference between the relic photons and relic neutrinos will widen.

2.2.2 Extrapolating the Current Energy of the Relic Neutrinos

The definition of cosmological redshift is: $1 + z \equiv a_{\text{now}}/a$, where $z_{\text{now}} = 0$ and a is the scale factor. The scale factor relates two points in space as space-time expands. The definition of the de Broglie wavelength is:

$$\lambda = \frac{h}{p} = \frac{hc}{\sqrt{E^2 - m^2c^4}} \tag{2.3}$$

I will be using subscripts γ and ν to signify photons and neutrinos respectively. Now, one can relate the redshift with the wavelengths by the fact that the change in wavelength is proportional to the scale factor, using units $\hbar = c = k_B = 1$,

$$1 + z_r = \frac{\lambda_n}{\lambda_r} \Rightarrow (1 + z_r)^2 = \frac{E_r^2 - m^2}{E_n^2 - m^2} \tag{2.4}$$

where the subscript r signifies the redshift when the neutrinos were ultra-relativistic and the subscript n signifies a redshift of zero. Using equation (2.4) for photons:

$$E_{\gamma n}(1 + z_r) = E_{\gamma r} \Rightarrow T_{\gamma n}(1 + z_r) = T_{\gamma r}, \tag{2.5}$$

since photons are massless their total energy is proportional to temperature. Now, relating the photon temperature at a redshift where the neutrinos are ultra-relativistic to the neutrinos' energy:

$$T_{\nu r} = \left(\frac{4}{11}\right)^{1/3} (1 + z_r) T_{\gamma n} \Rightarrow E_{\nu r} = T_{\nu r} + m_\nu. \tag{2.6}$$

The neutrinos' temperature is proportional to their kinetic energy, hence: $E_{\nu r} = T_{\nu r} + m_\nu$. Plugging equation (2.6) into equation (2.4) and solving for $E^2_{\nu n}$:

$$E^2_{\nu n} = \left(\frac{4}{11}\right)^{2/3} T^2_{\gamma n} + \frac{2}{(1+z_r)} \left(\frac{4}{11}\right)^{1/3} m_\nu T_{\gamma n} + m^2_\nu \tag{2.7}$$

Substituting $T_{\nu n} + m_\nu$ for $E_{\nu n}$ and solving for $T_{\nu n}$:

$$T_{\nu n} = \left(\left(\frac{4}{11}\right)^{2/3} T^2_{\gamma n} + \frac{2}{(1+z_r)} \left(\frac{4}{11}\right)^{1/3} m_\nu T_{\gamma n} + m^2_\nu \right)^{1/2} - m_\nu \tag{2.8}$$

If z_r is large, then the $1/(1+z_r)$ term can be neglected, this is an extremely good approximation since z_r is the redshift where neutrinos are ultra-relativistic. Taking the ultra-relativistic limit of the momentum, $p_r = E_r$, in equation (2.4) yields:

$$(1+z_r) = \frac{E_{\nu r}}{(E^2_{\nu n} - m^2_\nu)^{1/2}} = \frac{(4/11)^{1/3}\,(1+z_r) T_{\gamma n}}{(E^2_{\nu n} - m^2_\nu)^{1/2}} \tag{2.9}$$

The dependence on redshift drops out and the current relic neutrino temperature can be expressed as, $T_{\nu n} = \sqrt{(4/11)^{2/3} T^2_{\gamma n} + m^2_\nu} - m_\nu$. Since neutrino masses are unknown, only limits can be placed on the current temperature. The KamLAND experiment measured $|\Delta m^2_{21}| = 7.9^{+0.6}_{-0.5} \times 10^{-5}$ eV$^2/c^4$ [8]. From this result, if one takes the limit that one mass goes to zero, then the lower limit of the square of the other mass is 7.4×10^{-5} eV$^2/c^4$, which yields a lower limit on the more massive neutrino to be ~ 0.0086 eV$/c^2$. The MINOS experiment measured $|\Delta m^2_{32}| = 2.74^{+0.44}_{-0.26} \times 10^{-3}$ eV$^2/c^4$ [9]. In a similar fashion one finds the lower limit on the most massive neutrino to be ~ 0.584 eV$/c^2$. The parameters used for all plots and results are in table (2.1). Figure (2.7) illustrates

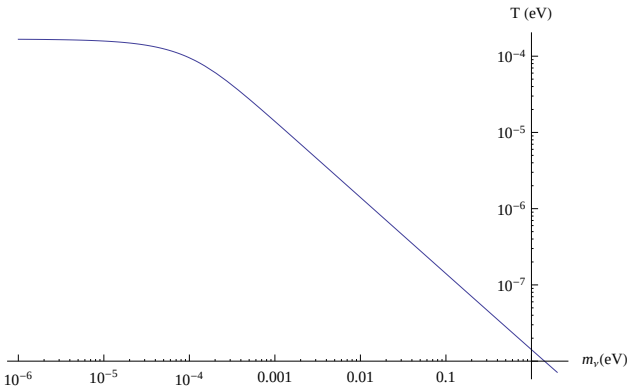

Figure 2.6: A log-log plot of $T_{\nu n}$ (in units of eV) as a function of m_ν/c^2.

Parameters and Results		
Varible	Value	Definiton
z_r	1.5×10^6	a redshift at which relic neutrinos were ultra-relativistic
$T_{\gamma n}$	0.235 meV $\simeq$ 2.725 K	current temperature of the CMB
m_{ν_2}	0.0086 eV	current lower bound of the m_2 neutrino mass
m_{ν_3}	0.0584 eV	current lower bound of the m_3 neutrino mass
$T_{m_{\nu_2}}$	0.019 K	current temperature of m_{ν_2}
$T_{m_{\nu_3}}$	0.0028 K	current temperature of m_{ν_3}
$m_{\mathrm{now}_{NR}}$	9.7×10^{-5} K	the mass of a neutrino where $E_\nu = 2m_\nu$ currently

Table 2.1: Results and parameters used to calculate the current temperature of the relic neutrinos.

temperature as a function of mass and shows that the correction to the relativistic limit for the lower limits on the neutrino masses is at least one to two orders of magnitude. Figure (2.8) show the redshift at which the temperature of the neutrinos is equal to the rest mass energy of the neutrinos. This is the regime where the neutrinos transition to behaving non-relativistically. From equation (2.4) we know that $(E_n^2 - m_\nu^2)(1 + z_{\mathrm{nonrel}})^2 = E_{\mathrm{nonrel}}^2 - m_\nu^2$, taking this and dividing it by $(E_n^2 - m_\nu^2)(1 + z_r)^2 = E_r^2 - m_\nu^2$ yields the expression:

$$(1 + z_{\mathrm{nonrel}})^2 = 3m_\nu^2(1 + z_r)^2/(E_r^2 - m_\nu^2), \tag{2.10}$$

where $E_{\mathrm{nonrel}} = 2m_\nu$. Even though it is beyond our current capability to measure the CνB, that does not preclude us from thinking about the implications or mean that it won't be measured in the future. The relic neutrinos provide a probe to $\sim$ 100 seconds after the big bang. This is a look back in time substantially larger than the CMB, which originated 380,000 years after the big bang. There is too much information in the CνB to not try to measure and understand it, and the first step toward that information is understanding the dynamics of the relic neutrinos.

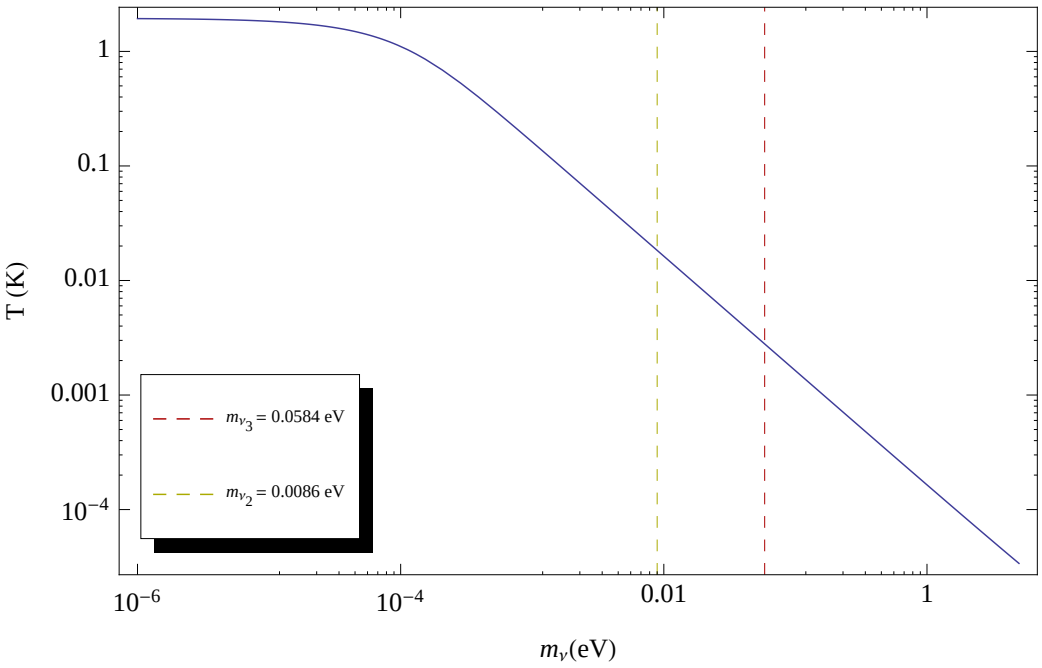

Figure 2.7: A log-log plot of $T_{\nu n}$ (in units of Kelvin) as a function of m_ν/c^2. The dashed lines are lower mass bounds on the two heaviest neutrino species, found from $|\Delta m^2|$ data.

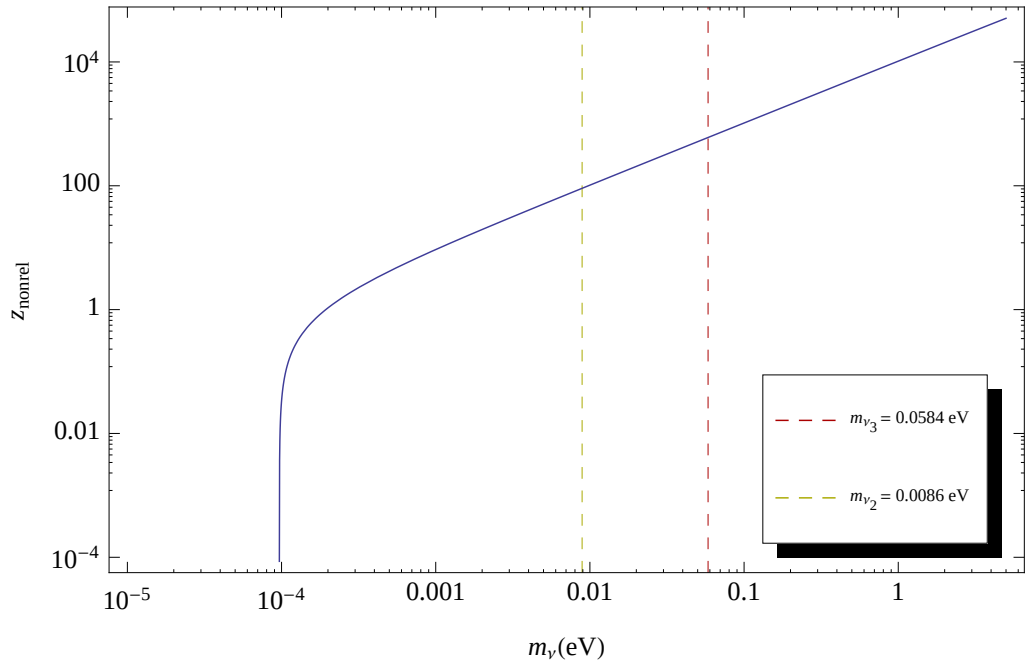

Figure 2.8: A log-log plot of the redshift where the neutrinos' kinetic energy equals their rest mass energy to its mass.

References

[1] L. Visinelli and P. Gondolo, arXiv:0810.4132v1 hep-ph, (2008).

[2] M. V. Medvedev, Journal of Physics A: Mathematical and Theoretical 43, 372002 (2010).

[3] R. Shankar, Principles of Quantum Mechanics (Springer, 1994).

[4] J. D. Jackson, Classical Electrodynamics (John Wiley & Sons Incorporated, 1999).

[5] M. V. Medvedev, Cosmological Simulations Evidence in Favor of Multi-Component Flavor-Mixed Cold Dark Matter, (2012).

[6] A. Kravtsov, Advances in Astronomy 2010, 1 (2010).

[7] E. W. Kolb and M. S. Turner, The Early Universe (Westview Pr, 1994).

[8] T. Araki, *et al*, Phys. Rev. Lett. 94, 081801. mult. p (2004).

[9] D. G. Michael, *et al*, Phys. Rev. Lett. 97, 191801 (2006).